Thermochimica Acta 520 (2011) 33–37

Contents lists available at ScienceDirect

Thermochimica Acta

journal homepage: www.elsevier.com/locate/tca

# Statistical continuum theory for the effective conductivity of carbon nanotubes filled polymer composites

M. Baniassadi[a,b], A. Laachachi[a,*], A. Makradi[a], S. Belouettar[a], D. Ruch[a], R. Muller[c], H. Garmestani[d], V. Toniazzo[a], S. Ahzi[b]

[a] Centre de Recherche Public Henri Tudor, AMS, 66 Rue de Luxembourg, BP 144 L-4002 Esch/Alzette, Luxembourg
[b] University of Strasbourg, IMFS, 2 Rue Boussingault, 67000 Strasbourg, France
[c] University of Strasbourg, ECPM, 25, rue Becquerel F-67087 Strasbourg, France
[d] School of Materials Science and Engineering, Georgia Institute of Technology, 771 Ferst Dr. N.W. Atlanta, GA 30332-0245, USA

ARTICLE INFO

*Article history:*
Received 21 September 2010
Received in revised form 21 February 2011
Accepted 27 February 2011
Available online 17 April 2011

*Keywords:*
Polymer nanocomposites
Statistical continuum theory
Effective thermal conductivity
Probability functions

ABSTRACT

The effective thermal conductivity of polymer nanocomposites filled with carbon nanotubes (CNTs) is studied using statistical continuum theory. A three-dimensional isotropic nanocomposite samples with randomly oriented CNTs are computer generated and used to calculate the effective thermal conductivity. The CNTs orientation, shape and spatial distribution are taken into account through two-point and three-point probability functions. The effect of filler content is studied by considering samples with filler contents vary form 1 to 10 wt%. The predicted effective conductivity is compared to our experiment, where the polymer matrix is taken to be poly(methyl methacrylate) (PMMA) filled with multiwalled carbon nanotubes (MWCNTs). Relative to the pure poly(methyl methacrylate) both the modeling and the experiment show an increase of the thermal conductivity as function of the MWCNTs volume fraction. However, the predicted results overestimate the experimental data, which might due the CNTs agglomerations. Therefore, the predicted effective conductivities have been compared to experimental results in order to estimate the volume fraction of CNT agglomeration.

© 2011 Elsevier B.V. All rights reserved.

## 1. Introduction

Polymers filled with carbon nanotubes (CNTs) result in lightweight nanocomposite materials with high mechanical and physical properties. The enhanced properties of Polymer/CNTs nanocomposites are attributed to the characteristic of CNTs such as shape and aspect ratio, as well as their orientation and distribution in the polymer matrix [1–3]. Hence, several experimental procedures and theoretical models are developed to guide producing nanocomposites with optimal properties. For instance, to take advantage of the fiber orientation effect on the physical properties of polymer/CNTs nanocomposites, different techniques have been developed to align CNTs in polymer matrix such as electrophoresis [4], mechanical stretching [5], hot filament chemical vapor deposition [6], melt processing [7] and high magnetic fields [8]. Regarding the effect of the CNTs distribution on the properties of nanocomposites, Kashiwagi et al. [9] showed that the enhancement of the physical properties of PMMA/SWCNT nanocomposites depends strongly on the degree of SWCNTs dispersion in the PMMA matrix.

Along with the experimental achievement in processing polymer/CNTs nanocomposites with optimized properties, several multi-scale theoretical models are developed to predict the effective properties of these nanocomposites. For instance, Deng et al. [10] developed an analytical model for thermal conductivity of CNTs nanocomposites with low loading of randomly oriented CNTs. This model takes into account the effect of the thermal conductive anisotropy and the influence of the aspect ratio. The results obtained indicate that larger aspect ratio improves the thermal conductivity for CNTs based nanocomposites. Ma and Gao [11] developed a three-dimensional Monte Carlo model to predict electrical conductivity of polymer matrix filled with curved nanofibers. The numerical results indicate that the composite conductivity decreases as the fibers become more curved and as the fibers aspect ratio decreases.

In this work, the strong-contrast approach [12,13] is used to predict the nanocomposites effective conductivity using a computer-generated three-dimensional nanocomposite structures. The distribution, shape and orientation distribution of the two phases are taken into account using two-point and three-point probability functions. The nanotubes percolation and local interaction between the nanotubes and the matrix are ignored. The predicted results are compared to our experimental results conducted on PMMA/MWCNT nanocomposites. These nanocom-

* Corresponding author. Tel.: +352 42 59 91 591; fax: +352 42 59 91 555.
*E-mail address:* Abdelghani.laachachi@tudor.lu (A. Laachachi).

0040-6031/$ – see front matter © 2011 Elsevier B.V. All rights reserved.
doi:10.1016/j.tca.2011.02.037

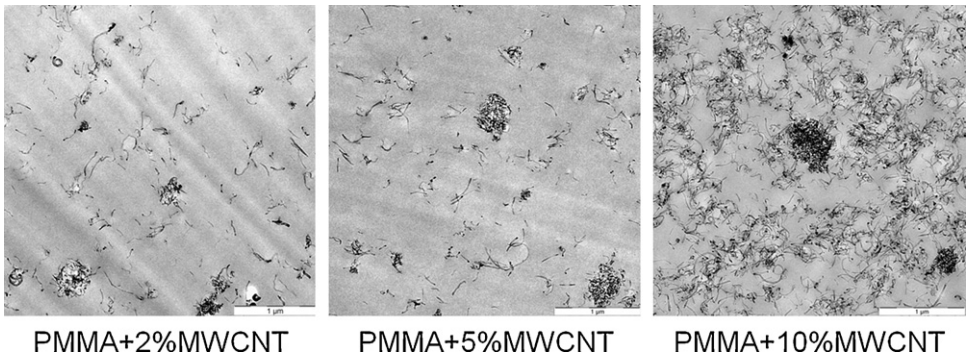


**Fig. 1.** TEM micrographs of PMMA/MWCNT nanocomposites.

posites are synthesized by melt mixing of the PMMA polymer with multiwalled carbon nanotubes (MWCNTs).

## 2. Experimental procedure and results

The goal of the experimental analysis conducted in this work is to evaluate the thermal conductivity ($\lambda(T)$) of the PMMA/MWCNT nanocomposites, as well as its dependence on the temperature. The thermal conductivity of PMMA/MWCNT nanocomposites can be deduced from the thermal diffusivity ($a(T)$), the specific heat ($Cp(T)$) and the bulk density ($\rho(T)$) according to the following equation:

$$\lambda(T) = \rho(T)Cp(T)a(T) \quad (1)$$

The physical parameters $\rho(T)$, $Cp(T)$ and $a(T)$ are measured from room temperature to 170 °C.

### 2.1. Materials

The polymer matrix used in this study is poly(methyl methacrylate) (PMMA) (Acrigel® DH LE, Mw = 78,000 g mol$^{-1}$ based on GPC analysis) which is supplied by Unigel Plasticos. The PMMA matrix is reinforced by multiwalled carbon nanotubes (MWCNTs), of purity superior to 90%, which might affects the dispersion of carbon nanotubes in the polymer matrix [14]. The MWCNTs are provided by Aldrich and used as received. The dimensions of the MWCNT range from 10 to 15 nm for the diameter and from 0.1 to 10 μm for the length.

### 2.2. Preparation of nanocomposites

The nanocomposites are prepared by melt mixing of the PMMA polymer with MWCNT using a twin-screw extruder (DSM Xplore). The PMMA and the MWCNT, at different contents (2, 5 and 10 wt%), are mixed at 230 °C for 7 min with a rotation speed of 200 rpm.

### 2.3. Characterization

Transmission electron microscopy (TEM) analyses of PMMA/MWCNT nanocomposites are carried out using a LEO 922 apparatus at 200 kV. These analyses are conducted on 70 nm thick films, prepared with a LEICA EM FC6 cryo-ultramicrotome at 25 °C. Fig. 1 shows the MWCNT dispersion into the PMMA matrix for three MWCNT volume fractions. The MWCNT are well distributed in the polymer matrix but with some tendency to aggregation, that increases with the concentration increase of the MWCNT. The size of the aggregates is much less than 500 nm.

Specific density $\rho(T)$ of the nanocomposite materials is determined using Archimedes' principle, where the volume is measured by the buoyancy in a fluid with known density. The weight and buoyancy measurements are performed with an electronic densimeter (X22B Wallace instrument). Pure water is chosen as fluid. The density measurements resolution is 0.001.

Specific heat $Cp(T)$ measurements are performed using a differential scanning calorimeter (DSC Netzsch 204 F1instrument). The measurements are carried out from 25 °C to 200 °C under a nitrogen flow and with a heating rate of 10 °C/min. The DSC is calibrated in the same temperature region before experiments, using a sapphire sample as standard, with a well-known specific heat. The deviation between the individual measurement results is generally less than ±2%.

Thermal diffusivity, $a(T)$, of the studied nanocomposites are measured by laser flash method. This technique entails heating the front side of a small, usually disk-shaped plane-parallel, sample by a short (≤1 ms) laser pulse. The temperature's increase on the sample rear surface is measured versus time using an infrared detector. Disk shaped samples, with a diameter of 12 nm and a thickness of 1 nm, are used to measure the thermal diffusivity under an Argon flow. All samples are molded under compression and coated, on both faces, with a very thin layer of colloidal graphite. The error for the thermal diffusivity measurement is evaluated at ±3%.

Relative to pure PMMA, MWCNT enhances the physical properties of the PMMA-based nanocomposites. However, the response to the temperature variation of the MWCNT/PMMA nanocomposites follows mainly the one of pure PMMA. To illustrate this behavior, the thermal diffusivity versus the temperature for PMMA and PMMA/MWCNT nanocomposites is reported in Fig. 2.

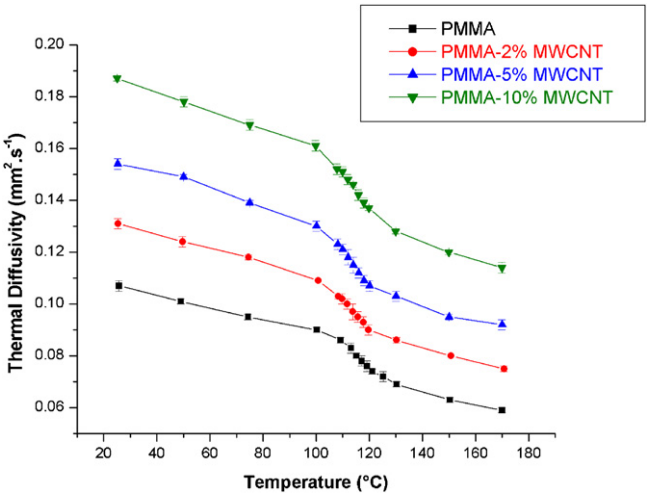


**Fig. 2.** Thermal diffusivity of PMMA and its nanocomposites with MWCNTs.

## 3. Formulation of the effective conductivity

### 3.1. Strong-contrast formulation

To derive the nanocomposite effective conductivity tensor $\lambda_e$, the MWCNT and the PMMA individual conductivities are assumed isotropic. Using the strong-contrast formulation of the statistical continuum theory, the effective conductivity is determined by resolving the following equation [12]:

$$\{\lambda_e - \lambda_R \boldsymbol{I}\}^{-1}\{\lambda_e + (d-1)\lambda_R \boldsymbol{I}\} = \frac{1}{\beta_{SR} P_1^S(\boldsymbol{x})}\boldsymbol{I} - \lambda_R d \int \left[\frac{P_2^S(\boldsymbol{x},\boldsymbol{x}') - P_1^S(\boldsymbol{x})P_1^S(\boldsymbol{x}')}{P_1^S(\boldsymbol{x})P_1^S(\boldsymbol{x}')}\right] \boldsymbol{H}^R(\boldsymbol{x}-\boldsymbol{x}')\,d\boldsymbol{x}' - \lambda_R^2 d^2 \beta_{SR} \iint \left[\frac{P_3^S(\boldsymbol{x},\boldsymbol{x}',\boldsymbol{x}'')}{P_1^S(\boldsymbol{x})P_1^S(\boldsymbol{x}')} - \frac{P_2^S(\boldsymbol{x},\boldsymbol{x}')P_2^S(\boldsymbol{x}',\boldsymbol{x}'')}{P_1^S(\boldsymbol{x})P_1^S(\boldsymbol{x}')P_1^S(\boldsymbol{x}'')}\right] \times \boldsymbol{H}^R(\boldsymbol{x}-\boldsymbol{x}')\cdot\boldsymbol{H}^R(\boldsymbol{x}'-\boldsymbol{x}'')\,d\boldsymbol{x}'\,d\boldsymbol{x}'' - \cdots \quad (2)$$

where $\boldsymbol{I}$ is the second-order identity tensor, $\beta_{SR}$ is the polarizability, $\lambda_R$ is the reference conductivity, and $\boldsymbol{H}^R(\boldsymbol{x}-\boldsymbol{x}')$ is a second-order tensor, defined below. The subscript R stands for the reference phase, which is chosen her to be the PMMA matrix, and the subscript/superscript S stands for the MWCNT phase.

The polarizability $\beta_{SR}$ is expressed by:

$$\beta_{SR} = \frac{\lambda_S - \lambda_R}{\lambda_S + (d-1)\lambda_R} \quad (3)$$

The second-order tensor $\boldsymbol{H}^R(\boldsymbol{x}-\boldsymbol{x}')$ is defined by:

$$\boldsymbol{H}^R(\boldsymbol{x}-\boldsymbol{x}') = \frac{1}{\Omega\lambda_R}\frac{d\boldsymbol{n}\boldsymbol{n} - \boldsymbol{I}}{(|\boldsymbol{x}-\boldsymbol{x}'|)^d} \quad (4)$$

where $\Omega$ is the total solid angle contained in a $d$-dimensional sphere and $\boldsymbol{n} = (\boldsymbol{x}-\boldsymbol{x}')/|\boldsymbol{x}-\boldsymbol{x}'|$.

$P_1^S(\boldsymbol{x})$, $P_2^S(\boldsymbol{x},\boldsymbol{x}')$ and $P_3^S(\boldsymbol{x},\boldsymbol{x}',\boldsymbol{x}'')$ are the probability functions that contain all microstructure informations, which will be developed the next subsection.

### 3.2. Probability functions

To take into account the statistical distribution and morphology of the microstructure, $n$-point probability functions are used. In case of two-phase materials, real $n$-point probability functions can be measured from micrographs representing the two-phase structure. Due to the complexity for calculating high probability functions, only one-point, two-point and three-point probability functions are determined and used to calculate the effective conductivity using Eq. (2). For instance, in a material composed of two phases, one-point probability function, $P_1^i(\boldsymbol{x}) = \phi_i$, is simply the volume fraction, $\phi_i$, for each phase ($i$). Two-point probably function, $P_2^{ij}(\boldsymbol{x},\boldsymbol{x}')$, measures the probability to find simultaneously a point $x$ in the phase ($i$) and a point $\boldsymbol{x}'$ in the phase ($j$). Fig. 3 recalls the definition of the position of the points $\boldsymbol{x}$ and $\boldsymbol{x}'$ in the cylindrical coordinates. In general, two-point probability functions can be used to measure the degree of homogeneity of heterogeneous two-phase materials. In fact, in case of homogenous two-phases materials, the value of the probability $P_2^{ii}(\boldsymbol{x},\boldsymbol{x}')$ tends to the volume fraction, $\phi_i$, of the phase $i$ once the point $x$ shifts close to $x'$ (i.e. $||\overrightarrow{\boldsymbol{x}\boldsymbol{x}'}|| = ||\vec{\boldsymbol{r}}|| \to 0$), and tends towards $\phi_i\phi_i$ once the distance $||\overrightarrow{\boldsymbol{x}\boldsymbol{x}'}||$ tends to infinity (i.e. $||\overrightarrow{\boldsymbol{x}\boldsymbol{x}'}|| = ||\vec{\boldsymbol{r}}|| \to \infty$):

$$P_2^{ij}(\boldsymbol{x},\boldsymbol{x}') = P_2^{ji}(\boldsymbol{x},\boldsymbol{x}') = 0,\ P_2^{ii}(\boldsymbol{x},\boldsymbol{x}') = \phi_i,\ P_2^{jj}(\boldsymbol{x},\boldsymbol{x}') = \phi_j \quad (5)$$

$$P_2^{ij}(\boldsymbol{x},\boldsymbol{x}') = P_1^i(\boldsymbol{x}) \times P_1^j(\boldsymbol{x}') = \phi_i\phi_j \quad (6)$$

Further, the homogeneity of the heterogeneous composite materials is a mandatory condition for the use of the statistical continuum theory to predict the physical properties of composite materials. In fact, for non homogeneous composite materials, the two-point probability functions does not verify the limits given in Eqs. (5) and (6), which lead to a non-convergence of the second and third terms on the right hand side of Eq. (2).

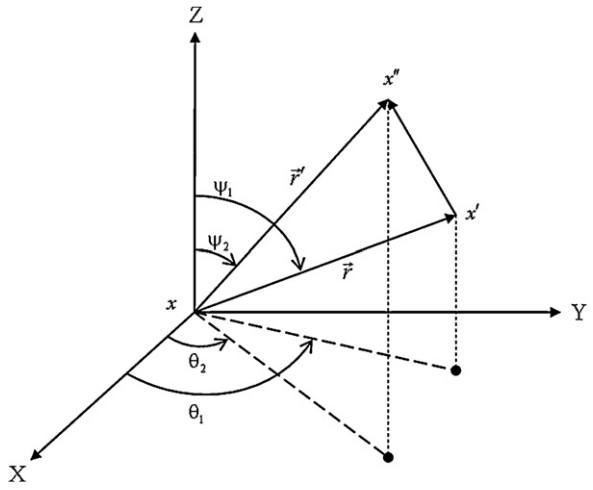


**Fig. 3.** Schematic representation of the vectors $\vec{\boldsymbol{r}}$ and $\vec{\boldsymbol{r}}'$ in spherical coordinates.

However, at the nanoscale, the micrographs reported in Fig. 1 are not homogeneous, and cannot be used in conjunction with the statistical continuum theory to predict their physical properties. Therefore to give an estimation of the physical properties of heterogeneous composite materials, three-dimensional MWCNTs filled PMMA nanocomposites with different MWCNTs content are computer generated. Fig. 4 shows a three-dimensional MWCNTs/PMMA with a MWCNTS volume fraction equal to 0.1, and the corresponding two-point probability functions are represented in Fig. 5. The two-point probability functions calculated from the nanocomposite represented in Fig. 4 verifies the limits given by Eqs. (5) and (6).

Regarding the three-point probability functions $P_3^{ijk}(\boldsymbol{x},\boldsymbol{x}',\boldsymbol{x}'')$, it can be determined by calculating the probability to find the points $\boldsymbol{x}$, $\boldsymbol{x}'$ and $\boldsymbol{x}''$ respectively in phases $i$, $j$ and $k$ (see Fig. 3). In a recent work by Mikdam et al. [13,15], an approximation for the three-point probability function was proposed and defined as follows:

$$P_3^{ijk}(\boldsymbol{x},\boldsymbol{x}',\boldsymbol{x}'') \cong \left(\frac{||\vec{\boldsymbol{r}}||}{||\vec{\boldsymbol{r}}|| + ||\vec{\boldsymbol{r}}'||}P_2^{ik}(\boldsymbol{x},\boldsymbol{x}'') + \frac{||\vec{\boldsymbol{r}}'||}{||\vec{\boldsymbol{r}}|| + ||\vec{\boldsymbol{r}}'||}P_2^{ij}(\boldsymbol{x},\boldsymbol{x}')\right) \times \frac{P_2^{jk}(\boldsymbol{x}',\boldsymbol{x}'')}{\phi_{j=k}}, \quad \text{with } j = k \quad (7)$$

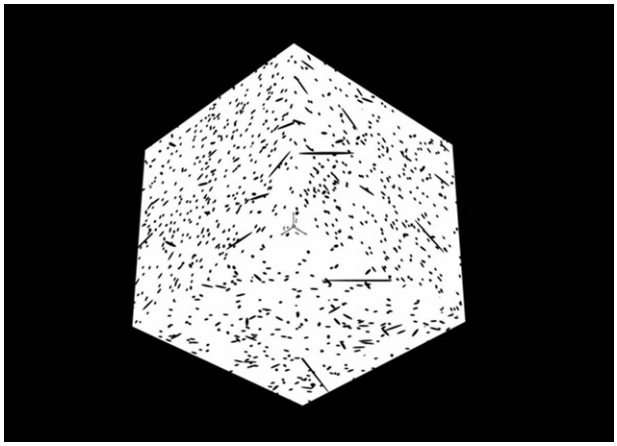

**Fig. 4.** Three-dimensional representation of carbon nanotubes–polymer nanocomposites.

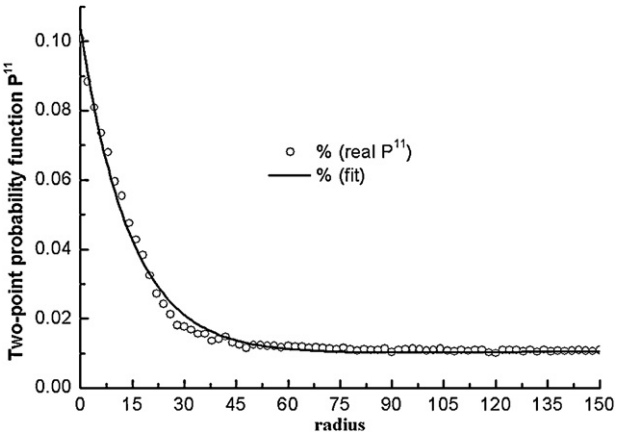


**Fig. 5.** Two-point probability functions of a 10% nanotubes–90% polymer nanocomposite.

where $||\vec{r}||$ and $||\vec{r}'||$ are distances, respectively, between $\boldsymbol{x}$ and $\boldsymbol{x}'$, $\boldsymbol{x}$ and $\boldsymbol{x}''$. In case of two-phase material, Eq. (7) verifies the three-point probability functions limits given by Torquato [12], and defined as follow:

$$\lim_{\substack{\overline{\boldsymbol{x}\boldsymbol{x}'} \to 0 \\ \overline{\boldsymbol{x}\boldsymbol{x}''} \to 0}} P_3^{i,j,k}(\boldsymbol{x}, \boldsymbol{x}', \boldsymbol{x}'') = \begin{cases} \phi_i & \text{if } i = j = k \\ 0 & \text{if not} \end{cases} \tag{8}$$

$$\lim_{\overline{\boldsymbol{x}'\boldsymbol{x}''} \to 0} P_3^{i,j,k}(\boldsymbol{x}, \boldsymbol{x}', \boldsymbol{x}'') = \begin{cases} 0 & \text{if } j \neq k \\ P_2^{ij}(\boldsymbol{x}, \boldsymbol{x}') & \text{if } j = k \end{cases} \tag{9}$$

$$\lim_{\substack{\overline{\boldsymbol{x}\boldsymbol{x}''} \to \infty \\ \overline{\boldsymbol{x}\boldsymbol{x}'} \text{ fixed}}} P_3^{i,j,k}(\boldsymbol{x}, \boldsymbol{x}', \boldsymbol{x}'') = \phi_k \times P_2^{ij}(\boldsymbol{x}, \boldsymbol{x}') \tag{10}$$

$$\lim_{\substack{\overline{\boldsymbol{x}\boldsymbol{x}'} \to \infty \\ \overline{\boldsymbol{x}\boldsymbol{x}''} \to \infty \\ \overline{\boldsymbol{x}'\boldsymbol{x}''} \to \infty}} P_3^{i,j,k}(\boldsymbol{x}, \boldsymbol{x}', \boldsymbol{x}'') = \phi_i \phi_j \phi_k \tag{11}$$

Fig. 6 shows the real three-point probability functions calculated from the 3D nanocomposite represented in Fig. 4 and compared to the one calculated from Eq. (7). Note that in Figs. 5 and 6 the nanotubes are denoted by phase (1) and the polymer matrix by phase (2)

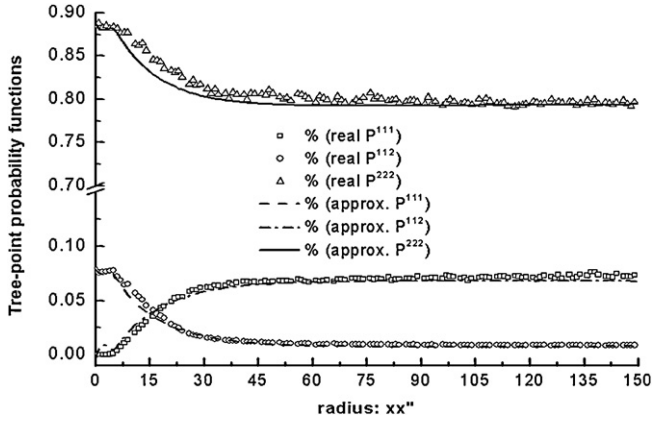


**Fig. 6.** Three-point probability functions of 10% nanotubes–90% polymer nanocomposite.

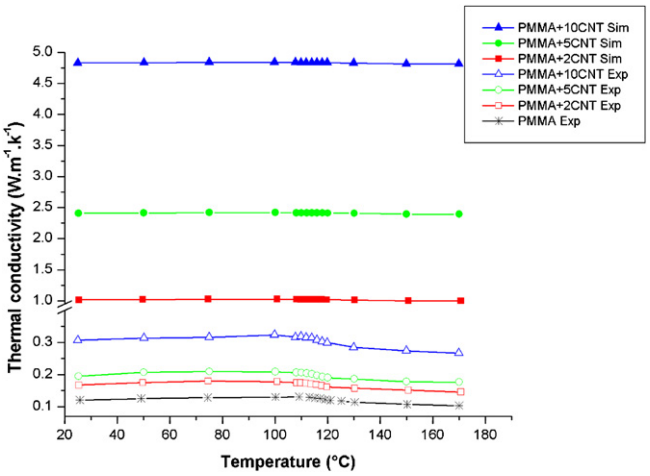


**Fig. 7.** Predicted thermal conductivity compared to experimental one for pure PMMA and PMMA/MWCNT nanocomposites.

## 4. Results and discussions

The effective conductivity of polymer nanocomposites filled with randomly distributed carbon nanotubes is calculated using the strong-contrast approach given in Eq. (7). The distribution, shape, orientation and aspect ratio of fibers are taken into account trough two-point and three-point probability functions (see Figs. 5 and 6). This approach can be used to evaluate the effective conductivity at macroscopically anisotropic composites consisting of isotropic phases. One of the salient aspects of this expansion is that when truncated at finite order, they give reasonably accurate estimation at rather all concentrations even though the contrast between the conductivities is high, like the contrast between the thermal conductivities of the polymer and carbon nanotubes in our simulations.

In our case, the conductivity of the PMMA matrix is represented by an isotropic conductivity given in Fig. 7 as function of the temperature. The conductivity of MWCNTs is taken isotropic equal to 200 W/mK, this value is measured using carbon nanotubes films [16]:

Fig. 7 shows the predicted and the experimental effective conductivity of the PMMA/MWCNT nanocomposites as function of the temperature for different MWCNTs volume fractions. It can be seen that, as expected, the thermal conductivity increases with the amount of MWCNT and slightly increases with increasing temperature between 25 and 110 °C. Around the glass transition temperature (115 °C), we observe a significant decrease in thermal conductivity of both PMMA and PMMA/MWCNT nanocomposites due to the motion of polymer chains.

The predicted conductivity overestimates the experimental one for each volume fraction of MWCNTs. Further the difference between the predicted and the experimental conductivities increases with the MWCNTs volume fraction. This behavior might due to the poor spatial dispersion of the MWCNTs in the PMMA matrix, as can be seen in Fig. 1. In fact, in case of PMMA/SWCNT nanocomposites, [9] show that higher spatial dispersion of SWCNTs leads to higher physical properties of the PMMA/SWNT nanocomposites. Furthermore, the increase of the fillers volume fraction leads to nanocomposites with higher agglomeration of the fillers (see Fig. 8). Therefore, more the fillers volume fraction is high more the spatial dispersion of the fillers is low, which might explain the increase of the discrepancy between the predicted and the experimental conductivity with the increase of the fillers volume fraction. Note that there might be other factors that contribute to this discrepancy between the modeling and the experiment such that

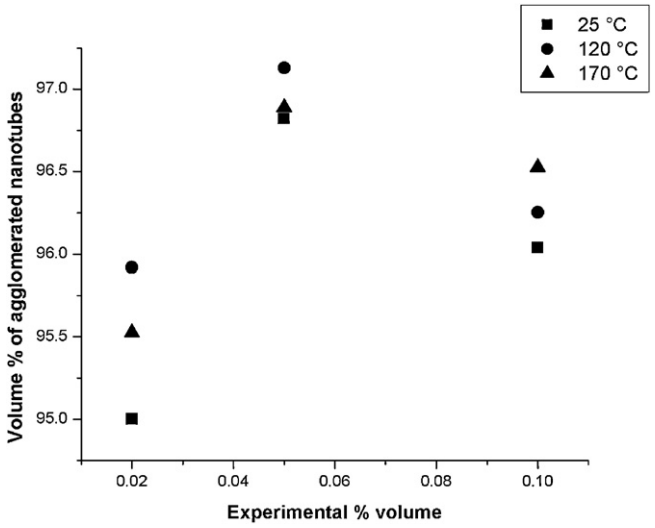


**Fig. 8.** Estimated volume percent of MWCNTs in PMMA matrix.

the nanotubes percolation, the anisotropy of the nanotubes property, the physics of nanotubes interactions and the interaction between the nanotubes and the polymer, which are ignored in this modeling.

## 5. Conclusions

Statistical continuum theory is used to predict the effective conductivity of multiwalled carbon nanotubes reinforced polymer matrix. The shape, orientation and distribution of each phase are accounted for using two-point and three-point probability functions. However, this modeling ignores the percolation and the interaction between the nanotubes and the polymer.

The polymer/CNTs nanocomposites are isotropic, due to the three-dimensional random distributed and orientation of the nanotubes in the polymer matrix. The individual conductivity of both the nanotubes and the polymer are taken isotropic. The predicted thermal conductivity overestimates the experimental one in case of PMMA/MWCNTs nanocomposites. Further the discrepancy between the predicted and the experimental results increase with the increase of the nanotubes volume fraction. This behavior might due to nanotubes aggregation, which tends to increase as the carbon nanotubes volume fraction increases.

## Acknowledgment

The authors would like to acknowledge the financial support from the Fond National de la Recherche (FNR) of the *Grand Duché of Luxembourg* (AFR Research Assistantship for Majid Baniassadi).

## References

[1] B.W. Smith, Z. Benes, D.E. Luzzi, J.E. Fischer, Structural anisotropy of magnetically aligned single wall carbon nanotube films, Applied Physics Letters 77 (2000) 663–665.
[2] T. Shokuhfar, A. Makradi, E. Titus, G. Cabral, S. Ahzi, A.C.M. Sousa, S. Belouettar, J. Gracio, Prediction of the mechanical properties of hydroxyapatite/polymethyl methacrylate/carbon nanotubes nanocomposites, Journal of Nanoscience and Nanotechnology 8 (2008) 4279–4284.
[3] Q. Wang, J. Dai, W. Li, Z. Wei, J. Jiang, The effects of CNT alignment on electrical conductivity and mechanical properties of SWNT/epoxy nanocomposites, Composites Science and Technology 68 (2008) 1644–1648.
[4] K. Yamamoto, S. Akita, Y. Nakayama, Orientation of carbon nanotubes using electrophoresis, Japanese Journal of Applied Physics 35 (1996) 917–918.
[5] L. Jin, C. Bower, O. Zhou, Alignment of carbon nanotubes in a polymer matrix by mechanical stretching, Applied Physics Letters 73 (1998) 1197–1199.
[6] Y. Chen, L. Guo, S. Patel, D.T. Shaw, Aligned conical carbon nanotubes, Journal of Materials Science 35 (2000) 5517–5521.
[7] R. Haggenmueller, H.H. Gommans, A.G. Rinzler, J.E. Fischer, Aligned single-wall carbon nanotubes in composites by melt processing methods, Chemical Physics Letters 330 (2000) 219–225.
[8] H. Garmestani, M.S. Al-Haik, K. Dahmen, R. Tannenbaum, D.S. Li, S.S. Sablin, M.Y. Hussaini, Polymer-mediated alignment of carbon nanotubes under high magnetic fields, Advanced Materials 15 (2003) 1918–1921.
[9] T. Kashiwagi, J. Fagan, J.K. Douglas, K. Yamamoto, A.N. Heckert, S.D. Leigh, J. Obrzut, F. Du, S. Lin-Gibson, M. Mu, K.I. Winey, R. Haggenmueller, Relationship between dispersion metric and properties of PMMA/SWNT nanocomposites, Polymer 48 (2007) 4855–4866.
[10] F. Deng, Q.S. Zheng, L.F. Wang, C.W. Nan, Effects of anisotropy, aspect ratio, and nonstraightness of carbon nanotubes on thermal conductivity of carbon nanotube composite, Applied Physics Letters 90 (2007) 021914.
[11] H.M. Ma, X.-L. Gao, A three-dimensional Monte Carlo model for electrically conductive polymer matrix composites filled with curved fibers, Polymer 49 (2008) 4230–4238.
[12] S. Torquato, Random Heterogeneous Materials: Microstructure and Macroscopic Properties, Springer, New York, 2002.
[13] A. Mikdam, A. Makradi, S. Ahzi, H. Garmestani, D.S. Li, Y. Remond, Effective conductivity in isotropic heterogeneous media using a strong-contrast statistical continuum theory, Journal of the Mechanics and Physics of Solids 57 (2009) 76–86.
[14] F. Du, J.E. Fischer, K.I. Winey, Coagulation method for preparing single-walled carbon nanotubes/poly(methyl methacrylate) composites and their modulus, electrical conductivity, and thermal stability, Journal of Polymer Science: Part B: Polymer Physics 41 (2003) 333–3338.
[15] A Mikdam, A. Makradi, S. Ahzi, H. Garmestani, D.S. Li, Y. Remond, A new approximation for the three-point probability function, International Journal of Solids and Structures 46 (2009) 3782–3787.
[16] D.J. Yang, Q. Zhang, G. Chen, S.F. Yoon, J. Ahn, S.G. Wang, Q. Zhou, Q. Wang, J.Q. Li, Thermal conductivity of multiwalled carbon nanotubes, Physical Review B 66 (2002) 1654401–1654406.